

## SHORT COMMUNICATIONS

# FLEXURAL CAPACITY OF EDGE LOADED ANNULAR FOUNDATIONS

SHASHIKANT SINGH<sup>1,\*</sup> AND KANAKAPURA S. SUBBA RAO<sup>2,†,‡</sup>

<sup>1</sup>*Department of Civil Engineering, North Eastern Regional Institute of Science and Technology, Itanagar, NIRJULI 791 109, India*

<sup>2</sup>*Department of Civil Engineering, Indian Institute of Science, Bangalore 560 012, India*

### SUMMARY

Edge loaded annular foundations have been analysed assuming the soil pressure at the contact to be non-uniform using the lower bound approach of Limit Analysis. Variable fixity at the edges has been allowed and the foundation slab is made to follow the Square yield criterion. Results presented in the form of curves can be readily used to obtain the locations of the yield hinge circles for the given slab and the corresponding collapse load. © 1997 by John Wiley & Sons, Ltd.

Int. J. Numer. Anal. Meth. Geomech., Vol. 21, 397–407 (1997)

(No. of Figures: 6    No. of Tables: 0    No. of Refs: 6)

Key words: annular foundation; collapse mode; contact pressure; lower bound; yield hinge circles; yield loads

### INTRODUCTION

Annular foundations are often provided below circular structures like towers and water tanks, wherein the loads are transferred to the foundation slab at both the inner and outer peripheries. Any study on foundation structures requires a method of analysis for the structural element along with a knowledge of the soil pressure distribution at the interface. Lower bound limit analysis is one of the well recognized methods which provides safe solutions for the collapse loads and also the details of the moment fields associated with the structure. Since the contact soil pressure is found to be non-uniform even for a symmetric loading system, it is realistic to adopt a model using a generalized paraboloid to represent the soil pressure at the interface.

Some upper bound solutions to the problem involving annular plates or slabs are available in the literature. The first correct upper bound solution for the yield point load for a simply supported annular plate obeying Tresca yield criterion was given by Hodge.<sup>1</sup> Identical upper and lower bound collapse loads for uniformly loaded simply supported and fixed

\* Assistant Professor Fax: 91-80-3341683, Tel.: 0845-8349 IISc IN

† Professor

‡ Correspondence to K. S. Subba Rao, Department of Civil Engineering, Indian Institute of Science, Bangalore 560 012, India

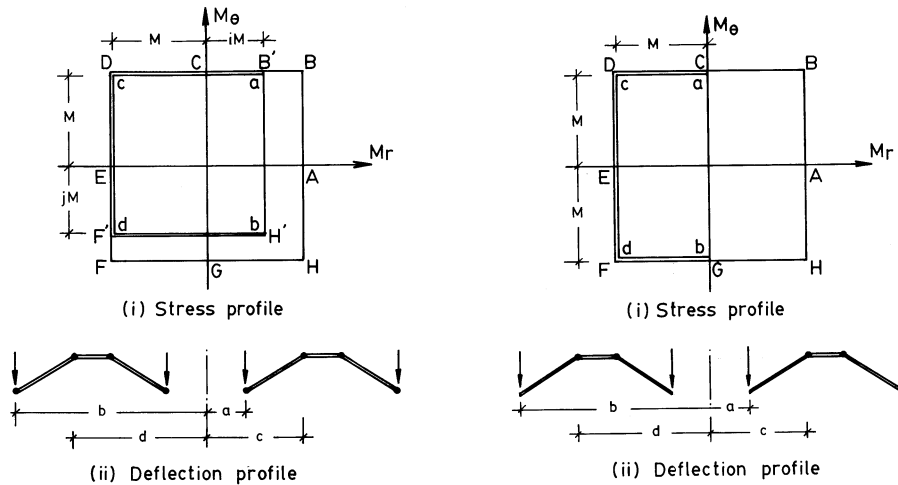


Figure 1. Moment regimes associated with square yield criterion (a) fixed edges ( $i \neq 0, j \neq 0$ ) (b) Simply supported edges ( $i = 0, j = 1$ )

annular slabs were presented by Ranganatham and Subba Rao<sup>2</sup> using the square yield criterion. Their solutions were found to be in agreement with the results obtained by Rozvany *et al.*<sup>3</sup> based on a different approach. Arya<sup>4</sup> considered the statics of annular foundation supporting a number of columns connected by a rigid beam at the base. The soil pressure was either uniform or linearly varying with the maximum compressive stress restricted to certain allowable limit and minimum pressure equally either zero or some compressive stress.

In the following, lower bound analysis for the load-carrying capacity of an edge loaded annular footing with variable fixity at the edges and resting on a general soil is presented. The slab element follows the Square yield criterion<sup>5</sup> of failure. In terms of principal moments  $M_r$  and  $M_\theta$ , defined as per Timoshenko and Krieger,<sup>6</sup> the square yield criterion follows the moment regime AB-CDEFGH as shown in Figure 1. In practice, the boundary conditions along the edges will be of either full or partial fixity. The analysis is carried out with allowance for different moment capacities in positive and negative zones and is capable of considering any level of fixity at the edges.

## ANALYSIS

The solution given by Hodge for the simply supported annular plate following Tresca yield criterion was an improvement upon an earlier incorrect solution presented by Chernina (vide Hodge<sup>1</sup>). It was demonstrated by Hodge that for the stress profile and the velocity fields to be both statically and kinematically admissible, there must exist two concentric and circular yield lines in the plate. Following the Hodge's conclusions, the deformed shape and the associated moment fields for an edge loaded annular footing obeying the square yield criterion will be as shown in Figure 1. There will be two hinge circles with a central rigid zone for both simply supported and clamped edge conditions.

*Boundary conditions*

- (i) For the zone bounded between the inner edge and the first yield circle, i.e., zone *ac* (Figure 1(a))

$$\begin{aligned} M_r &= iM & \text{at the inner edge, i.e., } r = a \\ M_r &= -M & \text{at } r = c \\ M_\theta &= M & \text{everywhere} \end{aligned} \quad (1a)$$

- (ii) For the zone bounded between the two hinge circles, i.e. zone *cd*,

$$\begin{aligned} M_\theta &= M & \text{at } r = c \\ M_\theta &= -jM & \text{at } r = d \\ M_r &= -M & \text{everywhere} \end{aligned} \quad (1b)$$

- (iii) For the zone bounded between the second hinge circle and the outer zone, i.e. zone *db*,

$$\begin{aligned} M_r &= -M & \text{at } r = d \\ M_r &= iM & \text{at } r = b \\ M_\theta &= -jM & \text{everywhere} \end{aligned} \quad (1c)$$

It can be noted that  $i = 0$  and  $j = 1$  in the above equations will represent a case of simply supported edges, shown in Figure 1(b).

*Contact pressure distribution*

The contact pressure distribution can be represented in two different forms. Depending upon the relative intensities of the loadings at the inner and outer edges and soil type, the pressure at the contact can be of continuously varying type with centre as the reference as shown in Figure 2(c) or it can have equal magnitude at both inner and outer edges as in Figure 2(d). The continuous distribution is expressed as

$$q(r) = q_0 \left[ n + (1 - n) \left\{ \frac{r}{b} \right\}^m \right] \quad (2)$$

and the second type is given by

$$q(r) = q_0 \left[ n + (1 - n) \left\{ \frac{2r - a - b}{b - a} \right\}^m \right] \quad (3)$$

where  $q_0$  is the soil pressure intensity at the edges and  $n$  is the ratio of the central pressure to the edge pressure. By varying the parameter ' $n$ ' distributions typical of different soil types ranging from sandy to clayey can be modelled. The collapse loads presented here are for the contact pressure represented by equation (2). The type represented by equation 3 can be dealt with by following identical steps.

**COLLAPSE LOADS**

Referring to Figure 2(a), the total load coming on the foundations is given by

$$W = 2\pi a P_1 + 2\pi b P_2 \quad (4)$$

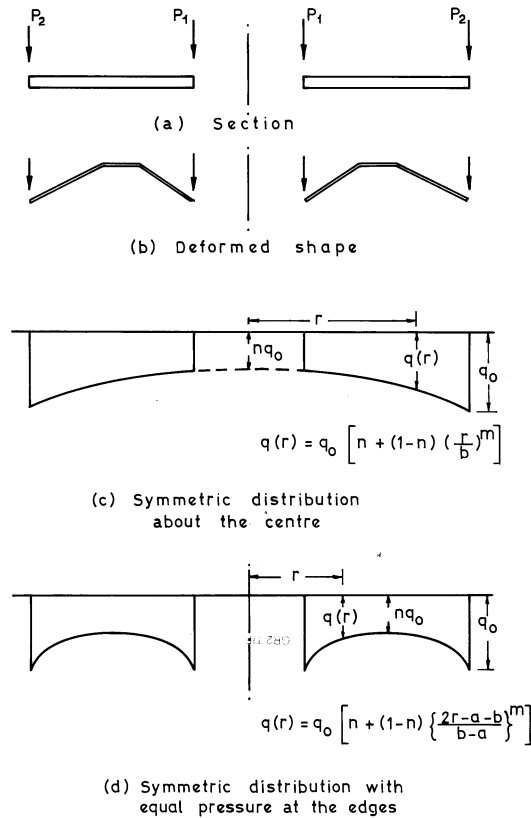


Figure 2. Types of soil pressure distribution for annular foundation

where  $P_1$  is the applied load per unit length at the inner edge, i.e. at  $r = a$ , and  $P_2$  is the applied load per unit length at the outer edge, i.e. at  $r = b$ .

The total soil reaction is expressed as

$$W = \int_0^{2\pi} \int_a^b q_0 \left[ n + (1-n) \left\{ \frac{r}{b} \right\}^m \right] r dr d\theta + 2\pi a Q_a + 2\pi b Q_b \quad (5)$$

where  $Q_a$  and  $Q_b$  are ring shears at the inner and outer edges and can be evaluated as follows.

Writing the equilibrium equations in terms of moments<sup>6</sup> as

$$\frac{d}{dr}(rM_r) - M_\theta = -rQ \quad (6a)$$

or

$$r \frac{d}{dr}(M_r) + (M_r - M_\theta) = -rQ \quad (6b)$$

To ensure that the moment  $M_r$  does not violate the yield condition inside the slab, in addition to the condition that at  $r = a$ ,  $M_r = iM$  and  $M_\theta = M$ ,  $M_r$  is permitted to attain a maximum only at

the edge in the inner zone by satisfying  $(d/dr)(M_r) = 0$  at  $r = a$ . Equation (6b), then, yields

$$Q_a = \frac{M}{a}(1 - i) \quad (7)$$

Similarly, at  $r = b$ , i.e. at the edge in the outer zone,  $M_r = iM$ ,  $M_\theta = -jM$  and  $(d/dr)(M_r) = 0$ , giving

$$Q_b = \frac{M}{b}(1 + j) \quad (8)$$

The shear given in equations (7) and (8) has not been accounted for by earlier investigators. The total load from equation (5) can now be expressed as

$$W = 2\pi q_0 b^2 \left[ \frac{n}{2} \left\{ 1 - \left( \frac{a}{b} \right)^2 \right\} + \frac{(1-n)}{(m+2)} \left\{ 1 - \left( \frac{a}{b} \right)^{m+2} \right\} \right] + 2\pi M(1 - 2i - j) \quad (9)$$

The shear equilibrium at any radius  $r$  is given as

$$2\pi r Q = 2\pi a P_1 - 2\pi a Q_a - \int_0^{2\pi} \int_a^r q_0 \left[ n + (1-n) \left( \frac{t}{b} \right)^m \right] t \, dt \, d\theta$$

or

$$rQ = aP_1 - aQ_a - q_0 \left[ \frac{n}{2} r^2 + \frac{(1-n)r^{m+2}}{(m+2)r^m} \right] + q_0 a^2 \left[ \frac{n}{2} + \frac{(1-n)}{(m+2)} \left( \frac{a}{b} \right)^m \right] \quad (10)$$

Integrating the moment equilibrium equation given in equation (6a) with equation (10), the moment field is obtained as

$$\begin{aligned} M_r - M_\theta = & -aP_1 + aQ_a + q_0 r^2 \left[ \frac{n}{6} + \frac{(1-n)}{(m+2)(m+3)} \left( \frac{r}{b} \right)^m \right] \\ & - q_0 a^2 \left[ \frac{n}{2} + \frac{(1-n)}{(m+2)} \left( \frac{a}{b} \right)^m \right] + \frac{C}{r} \end{aligned} \quad (11)$$

The constant  $C$  and the load  $P_1$  are evaluated for each zone by satisfying the boundary conditions as stipulated in equation (1). The moment fields for each of the three zones are obtained as follows:

*Zone ac*

$$\begin{aligned} aP_1 = & M \frac{(3-i)c - 2(1-i)a}{(c-a)} + q_0 a^2 \frac{c}{(c-a)} \left[ \frac{n}{6} \left\{ \left( \frac{c}{a} \right)^2 + 2 \frac{a}{c} - 3 \right\} \right. \\ & \left. + \frac{(1-n)}{(m+2)(m+3)} \left( \frac{a}{b} \right)^m \left\{ (m+2) \frac{a}{c} + \left( \frac{c}{a} \right)^{m+2} - m - 3 \right\} \right] \end{aligned} \quad (12)$$

$$\begin{aligned} M_r = & -M \left[ \frac{c(r-a)}{r(c-a)} \right] (1+n) - q_0 a^2 \left[ \frac{c(r-a)}{r(c-a)} \right] \\ & \times \left[ \frac{n}{6} \left\{ \left( \frac{c}{a} \right)^2 + 2 \frac{a}{c} - 3 \right\} + \frac{(1-n)}{(m+2)(m+3)} \left( \frac{a}{b} \right)^m \left\{ \left( \frac{c}{a} \right)^{m+2} + \frac{a}{c} (m+2) - m - 3 \right\} \right] \\ & + q_0 a^2 \left[ \frac{n}{6} \left\{ \left( \frac{r}{a} \right)^2 + 2 \frac{a}{r} - 3 \right\} + \frac{(1-n)}{(m+2)(m+3)} \left( \frac{a}{b} \right)^m \left\{ \left( \frac{r}{a} \right)^{m+2} + \frac{a}{r} (m+2) - m - 3 \right\} \right] \end{aligned} \quad (13)$$

and

$$M_\theta = M \quad (14)$$

Zone *cd*

$$aP_1 = M(3 - i) + q_0 \left[ \frac{n}{2}(c^2 - a^2) + \frac{(1 - n)}{b^m(m + 2)}(c^{m+2} - a^{m+2}) \right] \quad (15)$$

$$M_r = -M \quad (16)$$

and

$$M_\theta = M - q_0 \left[ \frac{n}{2}(r^2 - c^2) + \frac{(1 - n)}{b^m(m + 2)}(r^{m+2} - c^{m+2}) \right] \quad (17)$$

Zone *db*

$$\begin{aligned} aP_1 = & - \left[ \frac{M}{b - d} \right] [i(2b - d) + j(b - d) + (2d - b)] - q_0 a^2 \left[ \frac{b}{b - d} \right] \\ & \times \left[ \frac{n}{6} \left\{ 3 - \left( \frac{b}{a} \right)^2 - \frac{d}{b} \left\{ 3 - \left( \frac{d}{a} \right)^2 \right\} \right\} + \frac{(1 - n)}{(m + 2)(m + 3)} \left( \frac{a}{b} \right)^m \right. \\ & \left. \times \left\{ m + 3 - \left( \frac{b}{a} \right)^{m+2} - \frac{d}{b} \left\{ m + 3 - \left( \frac{d}{a} \right)^{m+2} \right\} \right\} \right] \quad (18) \end{aligned}$$

$$\begin{aligned} M_r = & -M \left[ \frac{d(b - r) - ib(r - d)}{r(b - d)} \right] + q_0 a^2 \left[ \frac{d(b - r)}{r(b - d)} \right] \\ & \times \left[ \frac{n}{6} \left\{ 3 - \left( \frac{b}{a} \right)^2 - \frac{d}{b} \left\{ 3 - \left( \frac{d}{a} \right)^2 \right\} \right\} + \frac{(1 - n)}{(m + 2)(m + 3)} \left( \frac{a}{b} \right)^m \right. \\ & \times \left\{ m + 3 - \left( \frac{b}{a} \right)^{m+2} - \frac{d}{b} \left\{ m + 3 - \left( \frac{d}{a} \right)^{m+2} \right\} \right\} \left. \right] - q_0 a^2 \\ & \times \left[ \frac{n}{6} \left\{ 3 - \left( \frac{r}{a} \right)^2 - \frac{d}{r} \left\{ 3 - \left( \frac{d}{a} \right)^2 \right\} \right\} + \frac{(1 - n)}{(m + 2)(m + 3)} \left( \frac{a}{b} \right)^m \right. \\ & \times \left\{ m + 3 - \left( \frac{r}{a} \right)^{m+2} - \frac{d}{r} \left\{ m + 3 - \left( \frac{d}{a} \right)^{m+2} \right\} \right\} \left. \right] \quad (19) \end{aligned}$$

and

$$M_\theta = -jM \quad (20)$$

### Collapse loads

The expressions for  $aP_1$  obtained from three zones must be equal and this condition is utilized in obtaining expressions for the collapse load in the respective zones. Equating equation (12) and

(15) and incorporating equation (9) the collapse load from the zone  $ac$  can be written as

$$\frac{W}{M} = \left[ \frac{2\pi\alpha(1+i) \left[ \frac{n}{2}(1-\alpha^2) + \frac{(1-n)}{(m+2)}(1-\alpha^{m+2}) \right]}{\frac{n}{6}(\alpha^3 + 2\beta^3 - \alpha\beta^2) + \frac{(1-n)}{(m+2)(m+3)}[\beta^{m+2}(\beta-\alpha)(m+2) - \alpha(\beta^{m+2} - \alpha^{m+2})]} \right] + 2\pi(1-2i-j) \quad (21)$$

For zone  $cd$ , the condition on  $M_\theta$  at  $r = d$  is utilized to get the collapse load. Equation (17) after incorporating equation (9) yields

$$\frac{W}{M} = \left[ \frac{2\pi(1+j) \left[ \frac{n}{2}(1-\alpha^2) + \frac{(1-n)}{(m+2)}(1-\alpha^{m+2}) \right]}{\frac{n}{2}(\eta^2 - \beta^2) + \frac{(1-n)}{(m+2)}(\eta^{m+2} - \beta^{m+2})} \right] + 2\pi(1-2i-j) \quad (22)$$

For zone  $db$  equation (18) is equated to equation (15) and with equation (9), the collapse load can be written as

$$\frac{W}{M} = \left[ \frac{2\pi[2+i-j-\eta(1+j)] \left[ \frac{n}{2}(1-\alpha^2) + \frac{(1-n)}{(m+2)}(1-\alpha^{m+2}) \right]}{\frac{n}{6}[1-\eta^3 - 3\beta^2 + 3\eta\beta^2] - \frac{(1-n)}{(m+2)(m+3)}[\eta^{m+3} + \beta^{m+2}(1-\eta)(m+3) - 1]} \right] + 2\pi(1-2i-j) \quad (23)$$

where  $W$  is the total collapse load,  $M$  is the moment capacity per unit length of the slab,  $\alpha$  is the ratio of the annulus radius to the outer radius, i.e.  $a/b$ ,  $\beta$  is the ratio of the radius of the first hinge circle to the outer radius, i.e.  $c/b$ ,  $\eta$  the ratio of the radius of second hinge circle to the outer radius, i.e.  $d/b$ .

Equations (21)–(23) are solved simultaneously for a given set of  $n, m, \alpha, i$  and  $j$  to get the values of the collapse load and the hinge circle spacings  $\beta$  and  $\eta$ . For a case of simply supported edges,  $i$  and  $j$  take the values zero and one, respectively, in the above equations.

## RESULTS

The collapse load equations have been solved numerically to obtain the magnitude of the collapse load and the yield circle locations following the steps indicated in the flow chart (Figure 3). Figure 4 shows the location of the yield circle for different  $\alpha$  values and contact pressure ratio  $n$  for a simply supported footing slab with continuous soil pressure distribution. Collapse loads are given for discrete values of  $\alpha$ ; the value at any intermediate point can be obtained by interpolation. Results show that the yield circle radii  $\beta$  and  $\eta$  increase with increasing  $\alpha$  and are more closely spaced to each other for higher values of  $\alpha$ . The collapse load, in general, increases with  $\alpha$ . Given the radius of the inner annulus and the type of the soil pressure, Figure 4 can be

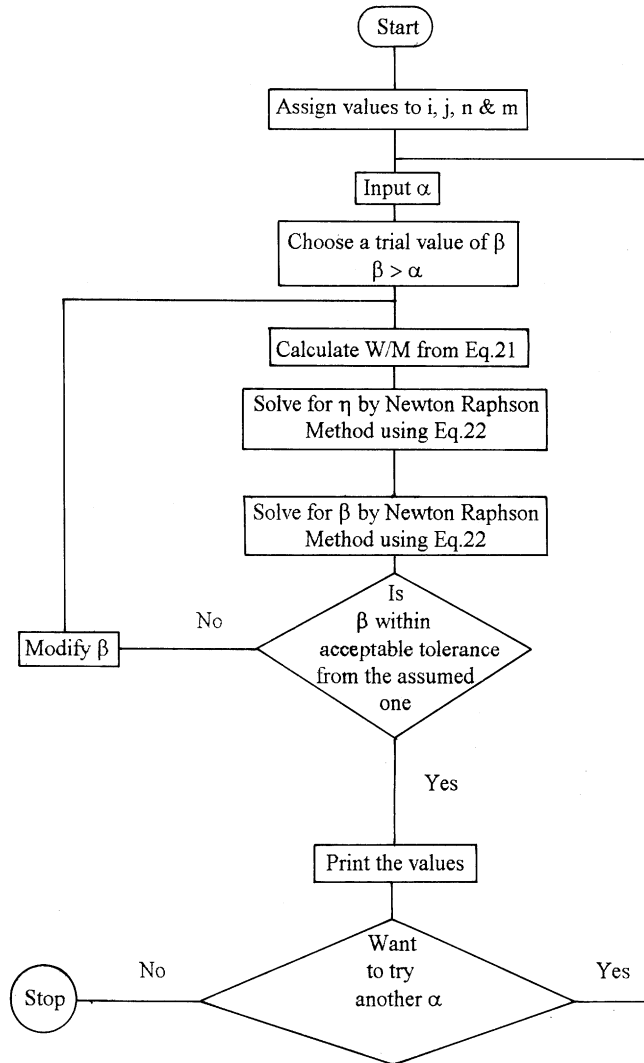


Figure 3. Flow chart for numerical computations

readily used to obtain positions of yield circles and the corresponding collapse loads. The variations of the collapse load with  $\alpha$  and  $n$  is contained in the discrete values at the top of the figure. It is seen that with higher values of  $n$  there is a decrease in the collapse load which can be explained in terms of the soil pressure resultant and the lever arm of the resulting couple in the particular zone. For smaller values of  $\alpha$ , in Figure 5, yield circles form nearer to the inner edge irrespective of  $n$ . As  $n$  increases,  $q_0$  at the outer edge being constant, the point of action of the resultant force shifts towards the inner edge. The outer zone, as a result, now has a larger lever arm and an increased pressure resultant, whereas the inner zone has a greater pressure resultant but a slightly reduced lever arm. The net effect is that with higher  $n$  a smaller load can induce a moment which equals the moment capacity of the slab at critical sections. For higher  $\alpha$ , the yield



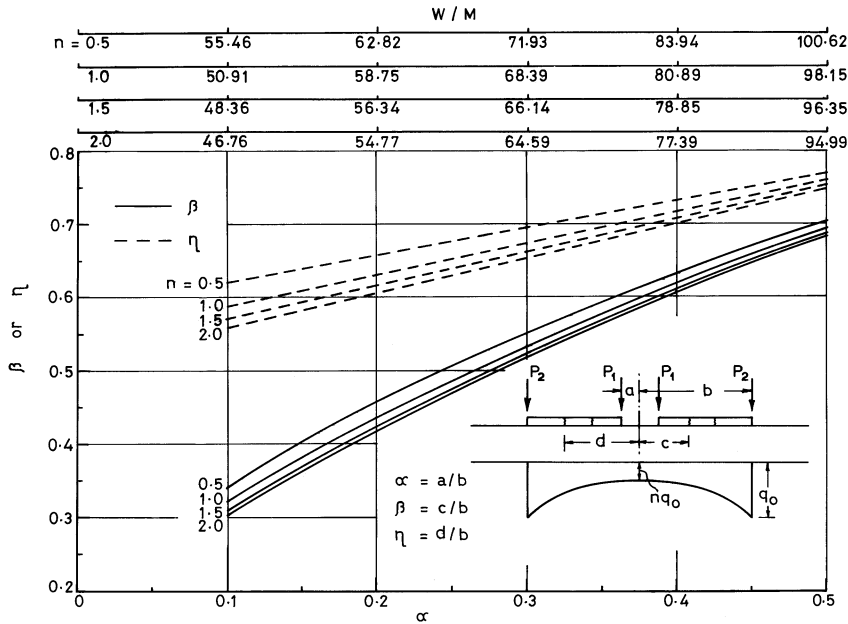


Figure 4. Collapse loads and yield hinge circle spacings for simply supported annular foundation with continuous soil pressure distribution

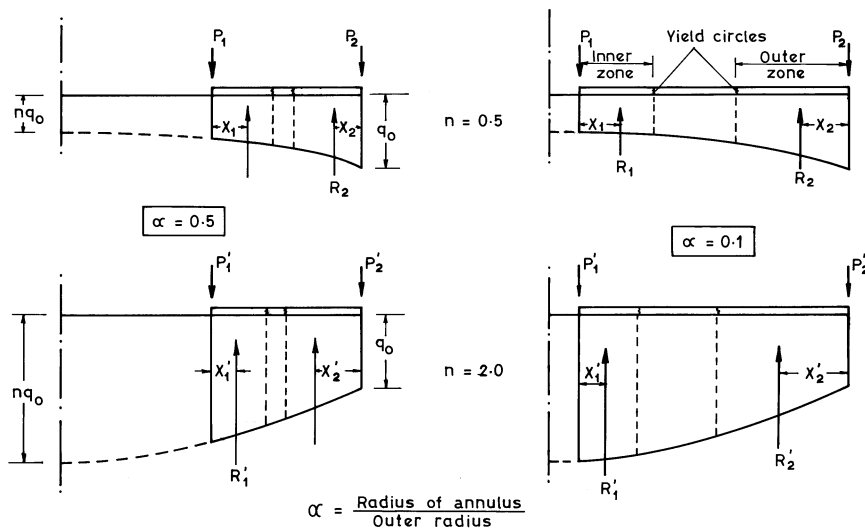


Figure 5. Formation of yield hinge circles and position of pressure resultants for different  $\alpha$

circles formation is affected to a greater extent by the variation in  $n$  because of the smaller size of the slab. The collapse load follows the same trend.

Figure 6 shows the collapse load variation and the hinge circle spacings for the footing slab with rotationally fixed edges but having the same pressure distribution as before. The plots are for

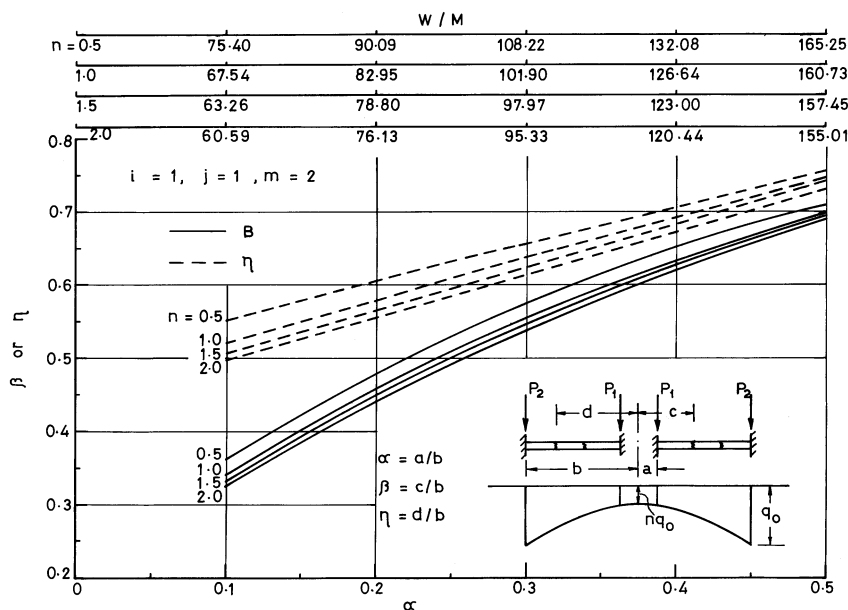


Figure 6. Collapse loads and yield hinge circle spacings for annular foundations with rotationally fixed edges and continuous soil pressure distribution

a second degree distribution and equal moment capacities in positive and negative direction. The collapse loads are found to be higher, and the increase, on an average over the range considered, is 48 per cent, the higher increase being 64 per cent and the lowest being 29 per cent when compared with the simply supported case. The yield circles form farther from the inner edge but are more closely spaced, the spacing being about 60 per cent of that of the simply supported case.

## CONCLUSIONS

Edge loaded annular foundations supported by non-uniform contact pressure distribution have been analysed to determine the collapse loads and the location of the yield hinge circles. Both simply supported and rotationally fixed end conditions have been considered. The complete lower bound collapse loads have been determined following the Square yield criterion. It has been ensured that the moment fields do not violate the yield conditions anywhere in the footing slab and the equilibrium equations are fully satisfied. The results presented in the form of curves can be readily used for determining the collapse load and the failure pattern for a given footing slab and soil condition; or for a given load and soil condition the same curves can be used to determine the moment capacity of the slab. Results show that the fixity at the edges increase the load carrying capacity of the foundation by about 48 per cent on an average for the soil pressure distribution under consideration. The yield hinge circles form closer together when the edges are fixed, with the spacing between them being about 60 per cent of that for the simply supported case.

## APPENDIX I

## Notations

$a$	radius of the annulus
$b$	radius of the outer periphery
$c$	radius of the first yield hinge circle
$d$	radius to the second yield hinge circle
$i, j$	fixity coefficients
$M$	field moment capacity per unit length of the slab
$M_r$	radial moment
$M_\theta$	circumferential moment
$m$	degree of the contact pressure distribution curve
$n$	ratio of the soil pressure intensity at the centre to that at the edge
$P_1$	load per unit length on the inner edge
$P_2$	load per unit length on the outer edge
$Q$	shear force per unit length
$q$	soil pressure
$W$	total collapse load
$\alpha$	ratio $a/b$
$\beta$	ratio $c/b$
$\eta$	ratio $d/b$

## REFERENCES

1. P. G. Hodge Jr., 'Yield point load of an annular plate', *J. Appl. Mech. Trans. ASME*, **26**, 454–455 (1959).
2. B. V. Ranganatham and K. S. Subba Rao, 'Limit analysis of annular slabs', *Int. J. Mech. Sci.* **14**, 693–699 (1972).
3. G. I. N. Rozvany, D. E. Charrett, S. R. Adidam and R. E. Melchers, 'A new approach to limit analysis', *J. Inst. Engrs., Australia Civil Eng. Trans.* **CE11**, 117–124 (1969).
4. A. S. Arya, 'Foundation of tall circular structures', *Indian Concrete J.*, **40**, 142–147 (1966).
5. R. H. Wood, *Plastic and Elastic Design of Slabs and Plates, with Particular Reference to Reinforced Concrete Slabs*, Thames and Hudson, London, 1961, p. 344.
6. S. Timoshenko and S. Woinowsky-Krieger, *Theory of Plates and Shells*, 2nd edn, McGraw-Hill, New York, 1959.